Theoretical and Applied Climatology (2021) 146:567–582
https://doi.org/10.1007/s00704-021-03756-0

ORIGINAL PAPER

Spatio-temporal analysis of land surface temperature for identification of heat wave risk and vulnerability hotspots in Indo-Gangetic Plains of India

Priyanka Rao[1] · Kshama Gupta[1] · Arijit Roy[1] · Raghunathan Balan[2]

Received: 3 November 2020 / Accepted: 12 August 2021 / Published online: 21 August 2021

Abstract
The increasing frequency of heat waves (HW) in many parts of the world is emerging as one of the climatic vulnerabilities across the world resulting in elevated thermal stress and high mortality. With increase in HW intensity, frequency and duration at global level, India has seen several major HW events in the last decade. HW conditions have mostly been studied by analysing ground-based observations; however, this approach lacks information on spatial variability at the local scale, which is not adequate to identify HW risk and vulnerability hotspots. In this study, gridded analysis of spatio-temporal variability of HW indices has been carried out by utilising freely available Moderate Resolution Imaging Spectrometer (MODIS) Land Surface Temperature (LST) data on Google Earth Engine (GEE) platform in the Indo-Gangetic Plains of India. HW indices to analyse duration, frequency and intensity of HW have been identified and further computed on a grid size of 10 km*10 km area. HW risk and vulnerability hotspot in the study region have been identified by spatial modelling of HW indices, LULC change and population density. The HW risk and vulnerability hotspot layer identified NCT Delhi and its surrounding region at the highest risk of HW with high vulnerability. A strong positive correlation of variability of HW indicators with increasing built-up shows that built-up surfaces affect strongly the HW conditions.

Keywords Heat wave · Hotspot · LST · Indo-Gangetic Plains · GEE

1 Introduction

Rising frequency of heat waves (HWs) is responsible for health hazards like thermal stress, a large number of deaths due to dehydration and adverse impact on the economy across the globe (IPCC, 2007; Meehl & Tebaldi, 2004). It has been established that an increase in greenhouse gases (GHG) due to intense anthropogenic activities is one of the key factors behind the increasing frequency and severity of HWs (Christidis et al., 2011). Recent HW events at a global level (Conti et al., 2005; Darryn et al., 2012; Luo & Zhang, 2012) have a significant impact on human health and mortality (Barriopedro et al., 2011; WMO, 2011). The impact is more profound in urban areas due to pre-existing urban heat island (UHI) effect, lack of vegetation cover and sheer density of population, which amplifies the impact of HW. Higher temperatures in urban areas intensify the perception of HW and associated thermal discomfort, resulting in higher mortality. Since urban areas are responsible for nearly three-fourth of GHG emission and house around 55% of the world population in 2–3% of total land area, mitigation measures in urban areas are important for extreme environmental hazards. Therefore, it is very important to spatially identify HW risk and vulnerability hotspots for detailed study and analysis as it will assist in framing local level strategies for mitigation and prevention of adverse impact on a large amount of population.

✉ Kshama Gupta
gupta.kshama@gmail.com

Priyanka Rao
priyanka123.iirs@gmail.com

Arijit Roy
arijitroy13@gmail.com

Raghunathan Balan
raghu15sep99@gmail.com

[1] Indian Institute of Remote Sensing, 4, Kalidas Road, Dehradun, Uttarakhand, India

[2] Birla Institute of Technology and Science – Pilani, Hyderabad Campus, Hyderabad, Telangana, India

HW is characterised as an abnormally hot weather condition for a prolonged period ranging from several days to weeks. Commonly used data to study heat waves are ground-based observations of ambient temperature (Mishra et al., 2017; Papanastasiou et al., 2014), but they do not provide spatial variability at finer scales, which is highly crucial to identify HW risk and vulnerability hotspots. One of the alternative data sets could be Moderate Resolution Imaging Spectrometer (MODIS) Land Surface Temperature (LST) data with daily day and night pass available continuously from the year 2003 onwards at 1-km ground resolution (Bahi et al., 2016). A significant number of studies have shown that LST is highly correlated with ambient temperature (Good et al., 2017; Kawashima et al., 2000; Bahi et al., 2016); hence, MODIS LST could be used as one of the best available proxies for ambient air temperature to study the spatio-temporal phenomenon of heat wave at a local scale.

The Indian subcontinent has seen a significant increase in temperature and HW events in the last few decades, resulting in considerable mortality (Pai et al., 2013). It is estimated that more than 20,000 people have died in India due to HW since 1990 (Mishra et al., 2017). India ranks at fifth place in the worldwide ranking with the death toll of 2081 persons per one hundred thousand population and gross domestic product (GDP) loss of 0.36% per unit due to volatile extreme weather events (Eckstein et al., 2019). HW frequency in India displayed a decadal increase of 25 in 1981–1990 to 67 in 2001–2010 (IMD, 2019; Rohini et al., 2016). The rise in temperature is getting more and more intense with increasing urbanisation and change in Land use Land Cover (LULC) (Rathee, 2014).

Indo-Gangetic Plains (IGP) of India is one of the largest river plains in the world and is amongst the most agriculturally productive regions of the world. It is also known as the food bowl of India and provides livelihood and food security for hundreds of millions of inhabitants (Seneviratne et al., 2012). It is one of the world's most densely populated areas housing approximately 1 billion people. It has also been observed that HWs are more frequent in IGP and HW metrics have shown significant intensification in IGP in the last few decades (Panda et al., 2017). Hence, in this study, MODIS LST available on Google Earth Engine (GEE) platform in analysis-ready format have been used to compute spatio-temporal variability of HW indicators and to identify the risk and vulnerability hotspots in the western IGP of India.

2 Study area

The study area selected for this research is part of IGP (Fig. 1). The study area falls under 2 major biogeographic zones of India and 6 agro-climate zones (out of total 16 zones). Biogeographic zones of India have been defined by the Wildlife Institute of India (WII) (Rodgers & Panwar, 1988), whereas agro-climatic zones are defined by the Indian Council of Agricultural Research (ICAR) (Mandal et al., 2016). The two biogeographic zones of India, selected as the study area, are Upper Gangetic Plains and Semi-arid Punjab Plains, which lie in the northern part of the country (Fig. 2a). The selected biogeographic zones fall under six agro-climatic zones of India, namely, Satluz-Yamuna Plain Region (semi-arid type of climate conditions), Upper-Ganga Plain Region (semiarid to subhumid climate with coarse loamy alluvial soils) some part of North-Western Mountain Region (cold arid type of climate with shallow skeletal soils),the Aravali Malwa Upland (hot semi-arid type of climatic conditions with medium and deep black soils), the middle-Ganga Plain (hot semiarid to sub-humid climatic characteristics with alluvial and Tarai soil type) and the western Rajasthan Region (hot semiarid climate with old alluvial soils) (Fig. 2b). It is evident that nearly 90% of the study area falls under three major agro-climate zones, namely Satluz-Yamuna Plain Region, Upper-Ganga Plain Region and middle-Ganga Plain, which has semi-arid climatic conditions with variation in humidity and soil conditions. The maximum temperature in the region during the summer goes up to 48℃ and the minimum temperature during the winter is 1℃. The annual average precipitation in this region ranges between 617 and 1667 mm. This area is highly urbanised and rich in agriculture as it has fertile soil. The region supports approximately 1/4th of total population of India according to census 2011. The LULC of this region is mostly dominated by agriculture. Moreover, it has been observed that this region has faced an increase in the HW frequency and intensity in last decade (Ghosh, 2020; Panda et al., 2017).

3 Materials and methods

3.1 Materials

The data used for identification of risk and vulnerability hotspots (Table 1) includes Aqua MODIS daily LST (https://earthengine.google.com/platform/) to compute the HW indicators, temporal LULC map (https://bhuvan-app1.nrsc.gov.in/thematic/thematic/index.php#) and population data from Global Human Settlement Layer (GHSL) (https://ghsl.jrc.ec.europa.eu/download.php?ds=pop).

Analysis-ready aqua MODIS LST product (daily pass 13:30 IST), available on GEE with a spatial resolution of 1 km, has been utilised for computation of HW indicators. One of the main challenges of using spatial data of high temporal frequency is the data volume and the huge storage and computation requirement. Computation of LST requires

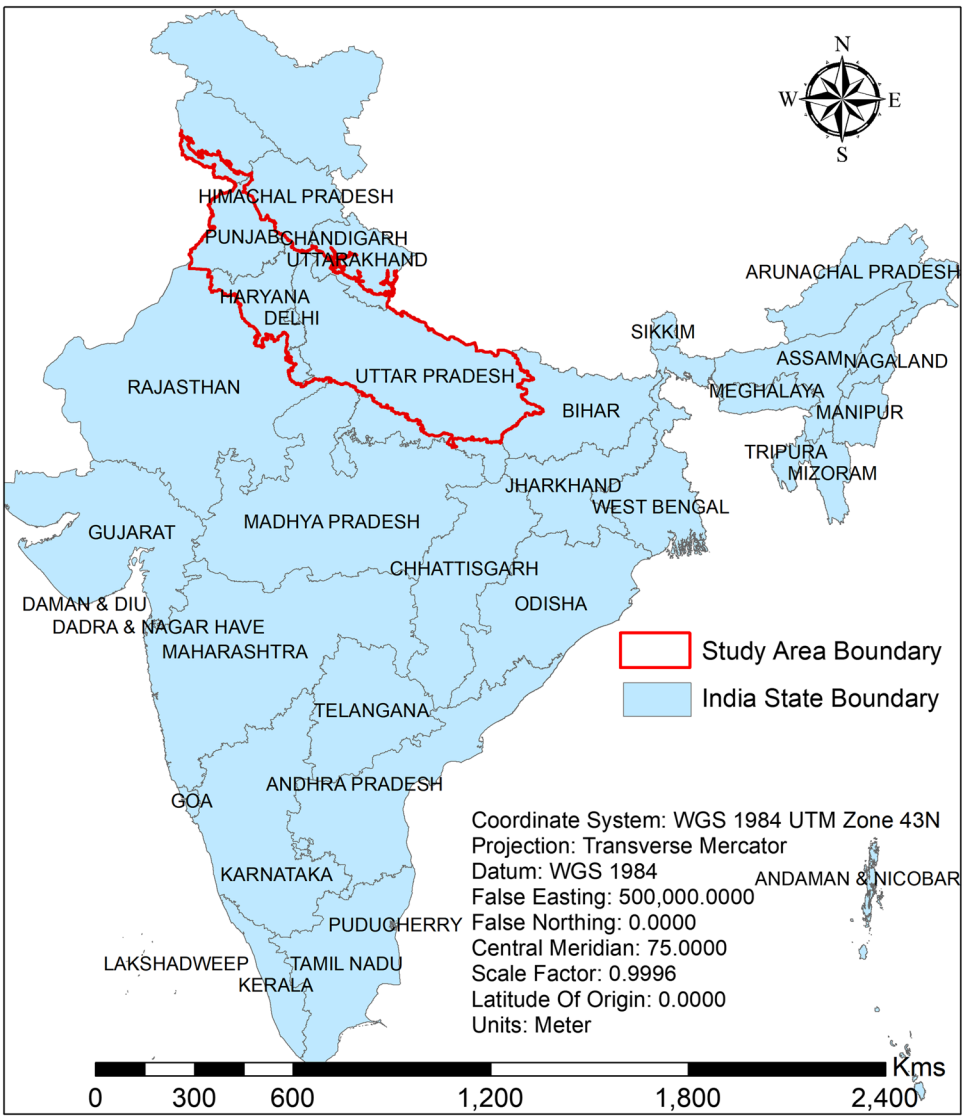

Fig. 1 Study area

long process with multiple steps for a single scene and it is highly computationally intensive to repeat the same process for large time series data, and requires dexterity to handle large volume of data. GEE is an open platform available freely to the user community. It provides access to remote sensing resources and a number of analysis-ready data products through its web portal. It allows a streamlined implementation of complex and large-scale workflows for processing and analysing the satellite data on the cloud, which also takes care of the data volume issues (Shelestov, et al., 2017). Hence, the GEE platform is employed in this study to analyse a large volume of LST data in one single step to compute HW indicators for any part of the world.

Bhuvan portal owned by National Remote Sensing Centre (NRSC), Hyderabad, India, provides ready-to-use temporal LULC for entire India (National Remote Sensing Agency, 2007; National Remote Sensing Centre, 2010). The LULC map has been generated using Advanced Wide Field Sensor (AWiFS) data aboard Indian remote sensing satellite Resourcesat 1 and 2 (spatial resolution of satellite data is 56 m). The LULC maps have been generated annually and available for use every 2-year interval at the Bhuvan portal. To analyse the land use transformation in the study area, LULC for the year 2005–2006, 2010–2011 and 2015–2016 has been obtained.

The grid wise population data has been obtained from the spatial raster datasets provided by European Commission, European Union Science Hub, GHSL. The data contains distribution and density of population, expressed as the number of people per cell, i.e. 1 km. It is one of the freely available datasets with significant spatial variation. The datasets are available for the four epochs, namely 1975, 1990, 2000 and 2015. Since the study period of this research is from 2003 to 2019, hence 2015 epoch data has been used for hotspot identification in this study.

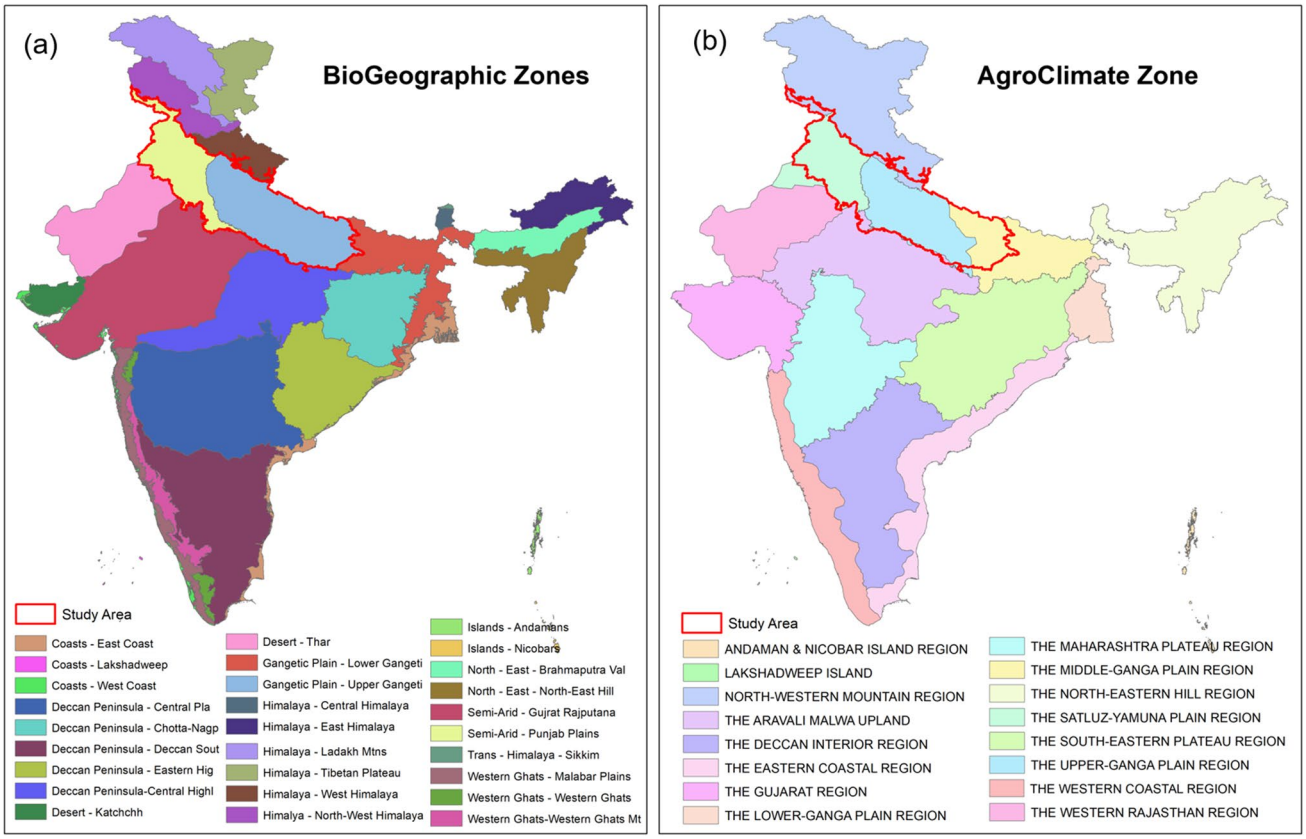

Fig. 2 (**A**) Biogeographic zones (source: Rodgers & Panwar, 1988) and (**B**) agro-climate zones (source: Mandal et al., 2016)

Table 1 Dataset used

Data type	Data source	Temporal resolution	Time period	Spatial resolution
Modis Aqua Land Surface Temperature (LST) Daily Product (day time)	Google Earth Engine (https://earthengine.google.com/platform/)	Daily (13:30 IST)	1Apr to 30Jun for year 2003 to 2019	1 km
Advanced Wide Field Sensor (AWiFS) Land Use Land Cover (LULC)	Bhuvan Portal (https://bhuvan-app1.nrsc.gov.in/thematic/thematic/index.php#)	Annual	2005–2006, 2010–2011, and 2015–2016	56 m
Population Layer (grid wise; total number of persons per sq. km.)	Global Human Settlement Layer (https://ghsl.jrc.ec.europa.eu/download.php?ds=pop)	Epoch	2015 epoch	1 km

3.2 Methods

Computation of various HW indicators has been carried out using MODIS LST products in GEE and python after identification of various HW threshold and indicators, which were integrated through analytical hierarchy process (AHP) to compute Cumulative HW Indicator. Since data volume was large, a software program in GEE and python was developed and executed for the computation of various HW indicators. Furthermore, risk and vulnerability hotspot has been identified by integrating Cumulative HW Indicators, LULC transformation layer and population data (Fig. 3).

3.2.1 Definition of heat wave

WMO Commission for Climatology (CCI) defined heat waves as: "A period of marked unusual hot weather (maximum, minimum and daily average temperature) over a

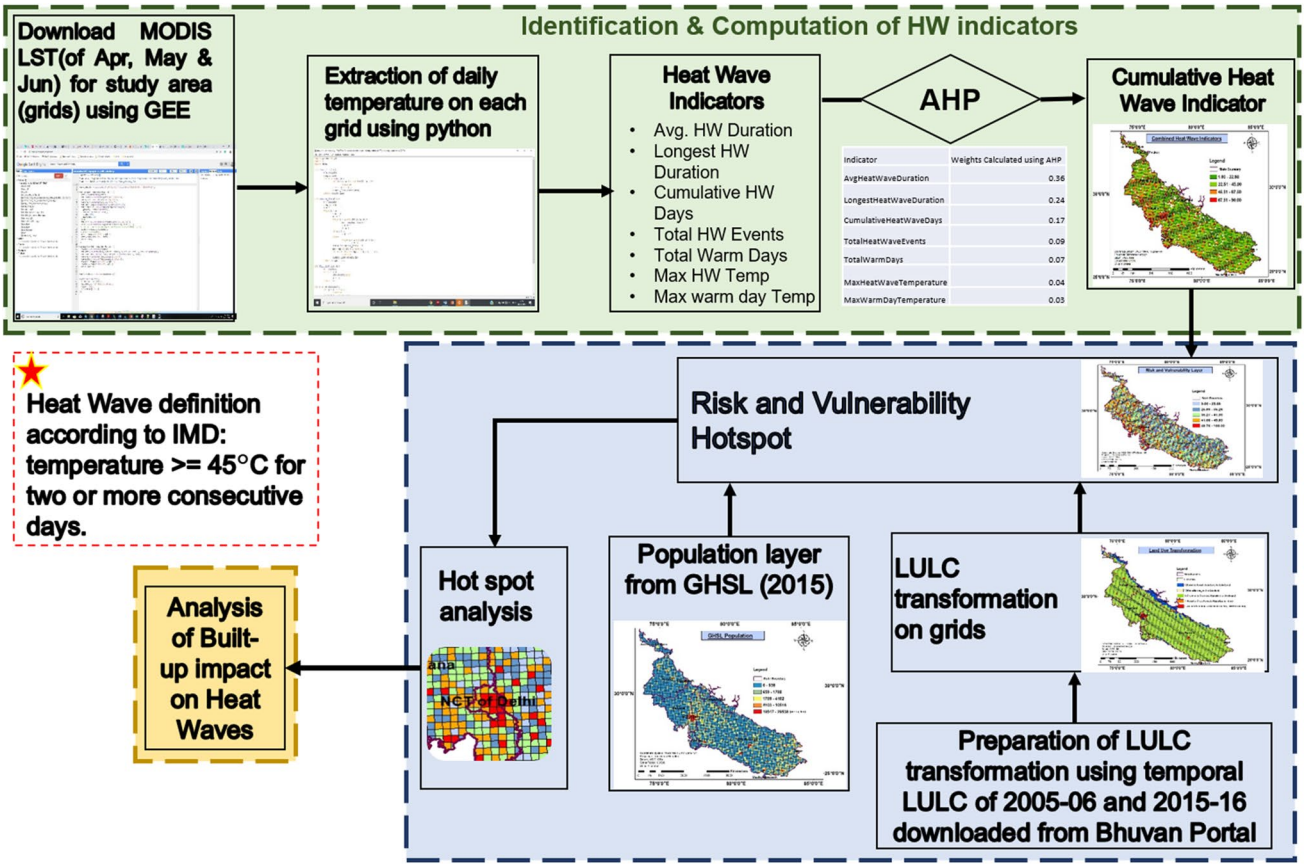

Fig. 3 Methodology adopted for hotspot analyses

region persisting at least three consecutive days during the warm period of the year based on local (station-based) climatological conditions, with thermal conditions recorded above given thresholds" (WMO, 2018). At a regional level, Indian Meteorological Department (IMD), India, has defined heat wave w.r.t. Indian Scenario as, "condition when the temperature reaches 45° C or beyond at least for 2 consecutive days, the weather condition shall be declared as heat wave". The HW definition given by IMD has been considered for this research work as the chosen study area falls in the Indian landscape.

3.2.2 Identification and computation of heat wave indicators

Identification of heat wave indices The World Meteorological Organization (WMO) in collaboration with several other climate and technical commissions has proposed eight HW indices that, alone or in combination, have been used for heat wave assessment/analysis for different regions (see http://etccdi.pacificclimate.org/list_27_indices.shtml). However, the indices given by the Expert Team on Climate Change Detection and Indices (ETCCDI) are based on absolute thresholds of extreme temperatures, which is suitable only for certain regions (Perkins, 2011). Due to various groups and sectors affected by the heat wave, of course, it is not possible to obtain the corresponding single index in each group which can be computed from the climatological data available. However, an adequate set of metrics providing information on various aspects of heat wave can be used for this purpose. Therefore, HW indicators used in this study thus identified are based on three main indicators of heat wave, i.e. duration, frequency and intensity (Table 2). The identified heat wave indices include Average HW Duration, Longest HW Duration, Cumulative HW Days, Total HW Events, Total Warm Day Events, Max HW Temperature and Max Warm Day Temp.

Data download using Google Earth Engine MODIS Aqua LST (MODIS/006/MYD11A1) day time product has been downloaded from GEE to obtain the daily LST for the 1 Apr to 30 Jun (maximum heat wave period) for seventeen consecutive years starting from 2003 to 2019. The time of pass was chosen as 1:30 PM IST instead of 10:30 AM IST as this is the peak solar insolation and temperature period.

Table 2 Different heat wave indicators along with identified indices

Heat wave indicator	Identified heat wave indices	Description	Source
Heat wave duration	Average Heat Wave Duration	Average duration of heat wave occurred in the month of Apr, May and Jun each year	(Alexander et al., 2006; Frich et al., 2002)
	Longest Heat Wave Duration (HWD)	Longest duration of heat wave amongst all the heat wave events observed in the Apr, May and Jun months of each year	(Frich et al., 2002; Shafiei Shiva et al., 2019)
	Cumulative Heat Wave Days (WSDI)	Total number of days under heat wave period occurred in the Apr, May and Jun months of each year	Alexander et al., (2006)
Heat wave frequency	Total Heat Wave Events	Total count of heat wave events occurred in Apr, May and Jun months of each year	(Frich et al., 2002; Meehl & Tebaldi, 2004; Shafiei Shiva et al., 2019)
	Total Warm Day Events	Total Warm days, when temperature went beyond 45 °C, irrespective of consecutiveness, in Apr, May and Jun months of each year	Frich et al., (2002)
Heat wave intensity	Maximum Heat Wave Temperature	Maximum temperature observed during heat wave period in Apr, May and Jun months of each year	(Khan et al., 2019; Meehl & Tebaldi, 2004)
	Maximum Warm Day Temperature	Maximum warm day temperature observed in Apr, May and Jun months of each year	(Khan et al., 2019; Shafiei Shiva et al., 2019)

Python code for extraction of temperature in each grid Computation of heat wave indicators was carried out at 10 km*10 km grids for the study area (Semi-arid Punjab Plains and Upper Gangetic Plains). Since HW is a phenomenon of extreme temperature for consecutive days, generalisation of values by calculating mean led to a loss in variability and identification of the actual HW period. Hence, the mode has been computed for each grid of 10 km *10 km. IMD defines HW as a period of temperatures above 45 °C for a minimum of at least 2 consecutive days, but simple statistical analysis as provided in GEE was not sufficient to identify the days with the temperature above 45 °C with a minimum of 2 consecutive days. Hence, a python code was developed in GEE to truncate the daily LST values below 45 °C. The csv file thus obtained from GEE was further categorised using a python code in order to identify the duration having temperature above the defined threshold for 2 consecutive days (Balan et al., 2020). The obtained data at each grid are then used for computation of HW indicators as identified earlier.

Computation of Heat Wave Indicators and Cumulative Heat Wave Indicator The HW duration between Apr and Jun has been added and divided by the total events of HW, to get the yearly Average HW Duration for each grid. Furthermore, to normalise the yearly Average HW Duration index into a single combined layer for further analysis, the Maximum Average HW Duration amongst all the 17 years has been assigned to each grid. Similarly, for each identified HW index, spatial heat wave index layers have been created. A cumulative index of HW has been computed by employing AHP to combine all seven heat wave indices to get the Cumulative Heat Wave index. Here, indices pertaining to duration have been given more weightage as more duration of HW exponentially increases adverse impact on human health, discomfort and mortality (Mazdiyasni et al., 2019). Further weightage has been given to frequency indices followed by intensity or temperature of the heat waves. The weights obtained after applying AHP on heat wave indices, viz. Average Heat Wave Duration, Longest Heat Wave Duration, Cumulative Heat Wave Days, Total Heat Wave Events, Total Warm Day Events, Maximum Heat Wave Temperature and Maximum Warm Day Temperature, were 0.36, 0.24, 0.17, 0.09, 0.07, 0.04 and 0.03 respectively (Table 3).

3.2.3 Identification of risk and vulnerability hotspot

To identify the risk and vulnerability hotspot, two layers of land use transformations and GHSL population layer have been combined with the Cumulative HW index. LULC maps obtained for the year 2005–2006 and 2015–2016 from the Bhuvan portal have been used to assess land use transformation, as land use plays a vital role in heat wave impact (Miralles et al., 2019). The classified LULC has 17 classes which were recoded into 5 major classes, viz. forest, built-up, cropland, waste/barren land and water, based on their

Table 3 Heat Wave indicators and calculated weights using AHP

Heat wave indicator	Weights calculated using AHP
Average Heat Wave Duration	0.36
Longest Heat Wave Duration	0.24
Cumulative Heat Wave Days	0.17
Total Heat Wave Events	0.09
Total Warm Day Events	0.07
Maximum Heat Wave Temperature	0.04
Maximum Warm Day Temperature	0.03

effect either positive or negative feedback on HW. Here, positive feedback means increment or more intensification to the heat wave phenomenon and negative feedback means contribution in decreasing the heat wave phenomenon. After the preparation of land use transformation layer, extraction of the land use transformation on the 10 km*10 km grids has been done by computing the median at each grid. All land use classes or categories have been given the ranking, on the scale of 1 to 9, where 1 represents the lowest and 9 as the highest positive feedback. The human population has been considered as one of the parameters to identify the heat wave risk and vulnerability hotspot, as the human population is one of the most important and valuable resources (Pal & Eltahir, 2016). Grid wise human population layer has been obtained from GHSL at 1-km resolution and it has been extracted on the grid shape file of the study area. All the parameter layers (heat wave indices, land use transformation and population), considered for the analysis of risk and vulnerability hotspot w.r.t. heat wave, were combined altogether by giving them equal weightage. Agro-climatic zone map was further used for the analysis of HW phenomenon in the study area.

3.2.4 Impact of built-up change on heat waves

The relationship between increased built-up and HW has been studied by extracting built-up area from the LULC of 2005–2006, 2010–2011 and 2015–2016 (downloaded from Bhuvan portal). The extracted built-up was then analysed with each HW indicator by considering 2005 as the base year.

4 Results

4.1 Heat wave indicators

All the HW indices based on major HW indicators, namely duration, frequency and intensity (Table 2), have been analysed for 17 years from 2003 to 2019 based on daily LST and have been normalised into a single layer for each HW index (Fig. 6). It can be seen that the Average HW Duration shows a greater percentage of grids under the highest range (5 and above) in the year 2019 (8.16%) than in the year 2009 (1.28%) (Fig. 4). It has also been observed that the area coming under the middle range (3–4) of this index increased in the decade of 2010–2019 compared to its previous decade. A similar pattern can be seen with the Longest HW Duration index (Fig. 4). The percentage of grids falling under the highest range, i.e. 10 and above in the last decade is 1.03% whereas between 2010 and 2019, this number reached to 2.36% which is significantly high as compared to 1.03%. Cumulative HW Days index (Fig. 4) also shows the similar pattern and a greater number of grids falls in the highest (23 and above), second highest (16–22) and the third highest (9–15) class during 2010–2019 decade. Total HW Events (Fig. 5) show the same pattern of the higher percentage of grids under the maximum range, i.e. 7 and above. It also shows the noticeable increase in the number of grids every year in the 2010–2019 decade in the highest (7 and above) and second highest (5–6) class. Total Warm Day Events (Fig. 5) revealed that 7 years between 2010 and 2019 decade, a considerable percentage of area under the highest range of this index, i.e., 29 and above, was recorded, whereas in the 2000–2009 decade, only 4 years could be observed with similar criteria. In the detailed graphical analysis (Fig. 5) for the percentage distribution of grids of Maximum HW Temperature, it has been observed that during the2000–2009 decade, only 2.11% out of the total area was under the temperature range of 58.01–64.00 °C, while it increased up to 9.85% in the 2010–2019 decade, which is comparatively very high. Maximum Warm Day Temperature (Fig. 5) also shows the yearly increase and consistent higher percentage of grids falling under the maximum range of temperature in the 2010–2019 decade.

The spatial distribution of normalised values of all the HW indices for the entire study period shows (Fig. 6) that mostly the southern part and Haryana and Delhi regions of the study area witnessed higher values of all the indicators. Cumulative HW index computed by applying AHP (Fig. 7) also provides the similar pattern where the region of NCT Delhi and the nearby area along with the neighbouring plains in the state of Haryana has higher values of heat wave index.

4.2 Risk and vulnerability hotspot

It can be clearly observed from the land use transformation map (Fig. 8) that the NCT Delhi region provides the highest positive feedback to heat waves due to significant changes in land use from agriculture to built-up area. The population distribution in the study area (Fig. 9) also shows the highest concentration of population in this region. Final risk

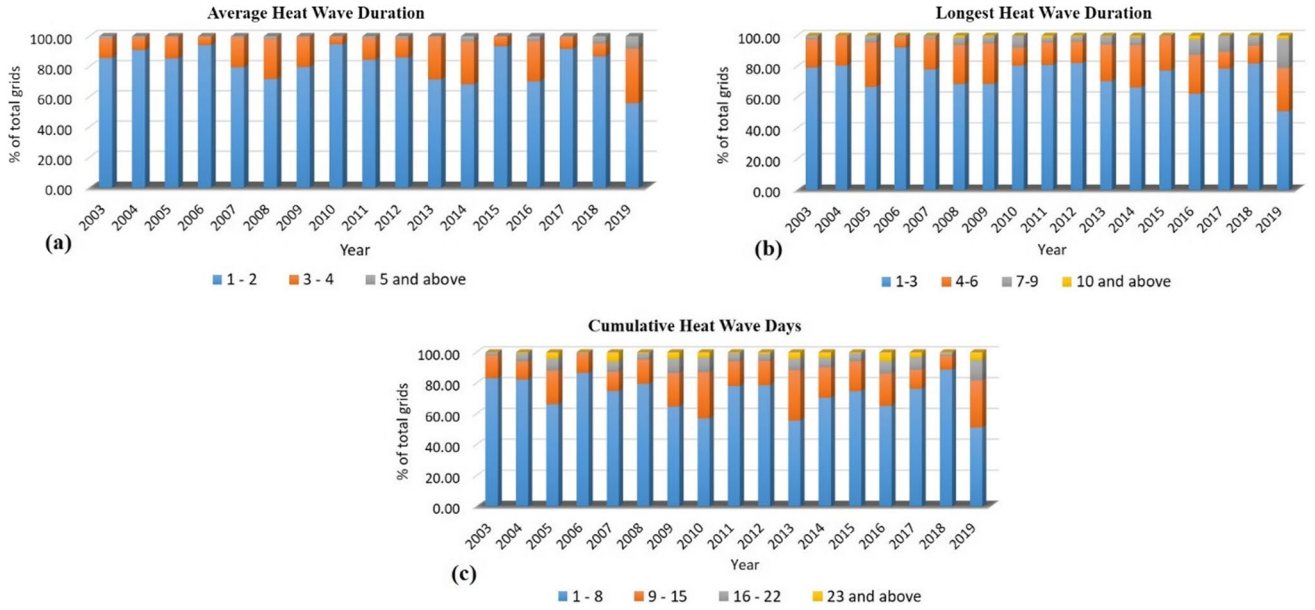

Fig. 4 Year wise analyses of grids falling under different range of identified heat wave duration indices. (a) Average Heat Wave Duration is the average duration of HW while, (b) Longest HW Duration is the longest HW period and (c) Cumulative HW Days are total days falling under HW period every year. They all indicate duration. Only Apr, May and Jun months of every year have been considered to calculate these heat wave indices

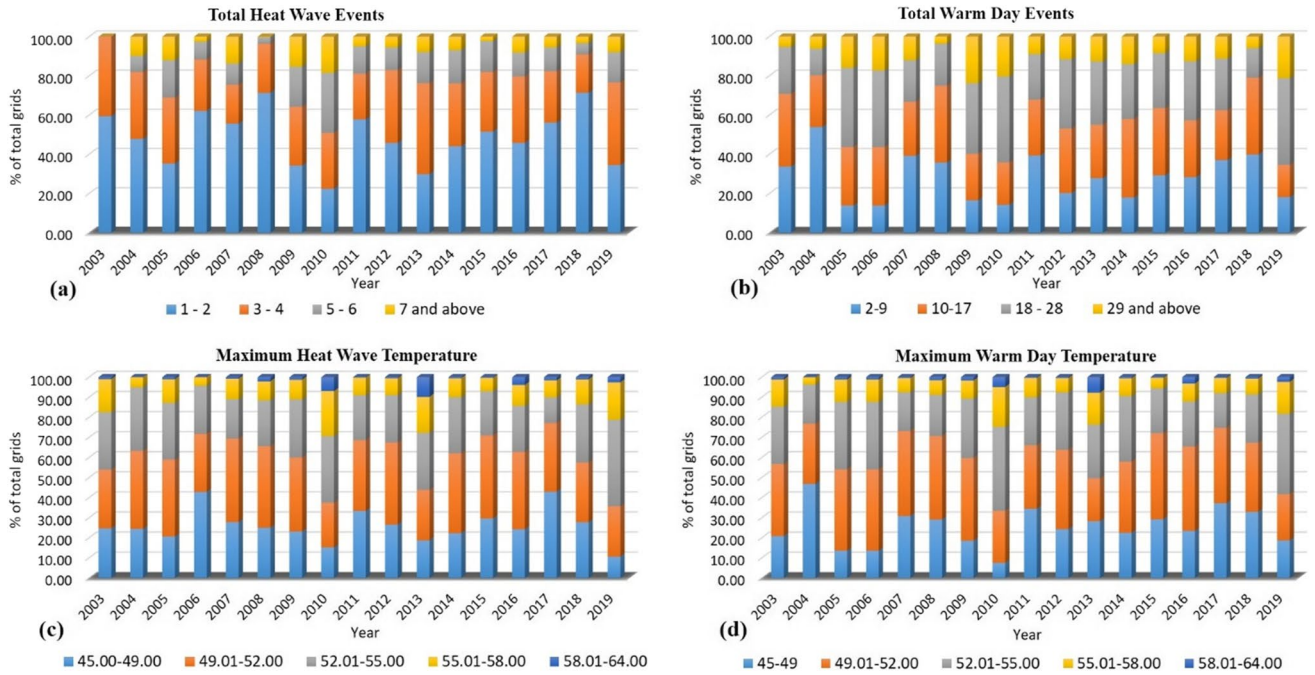

Fig. 5 Year wise analyses of grids falling under different range of identified heat wave frequency and intensity indices. (**a**) Total HW Events are sum of HW events that occurred in each year, whereas (**b**) Total Warm Day Events are total warm days that occurred every year. They ((**a**) and (**b**)) both indicate heat wave frequency. (**c**) Max HW Temp is max temp recorded in HW period, and (**d**) Max Warm day Temp is max temp recorded every year. They ((**c**) and (d**d**)) indicate HW intensity. Only Apr, May and Jun months of every year have been considered for the calculation of all the heat wave indices

and vulnerability layer (Fig. 10) after the integration of HW indicator, land use transformation and population, identify NCT Delhi and its surrounding region as one of the areas at highest risk of HW events. Some pockets (grids) have also

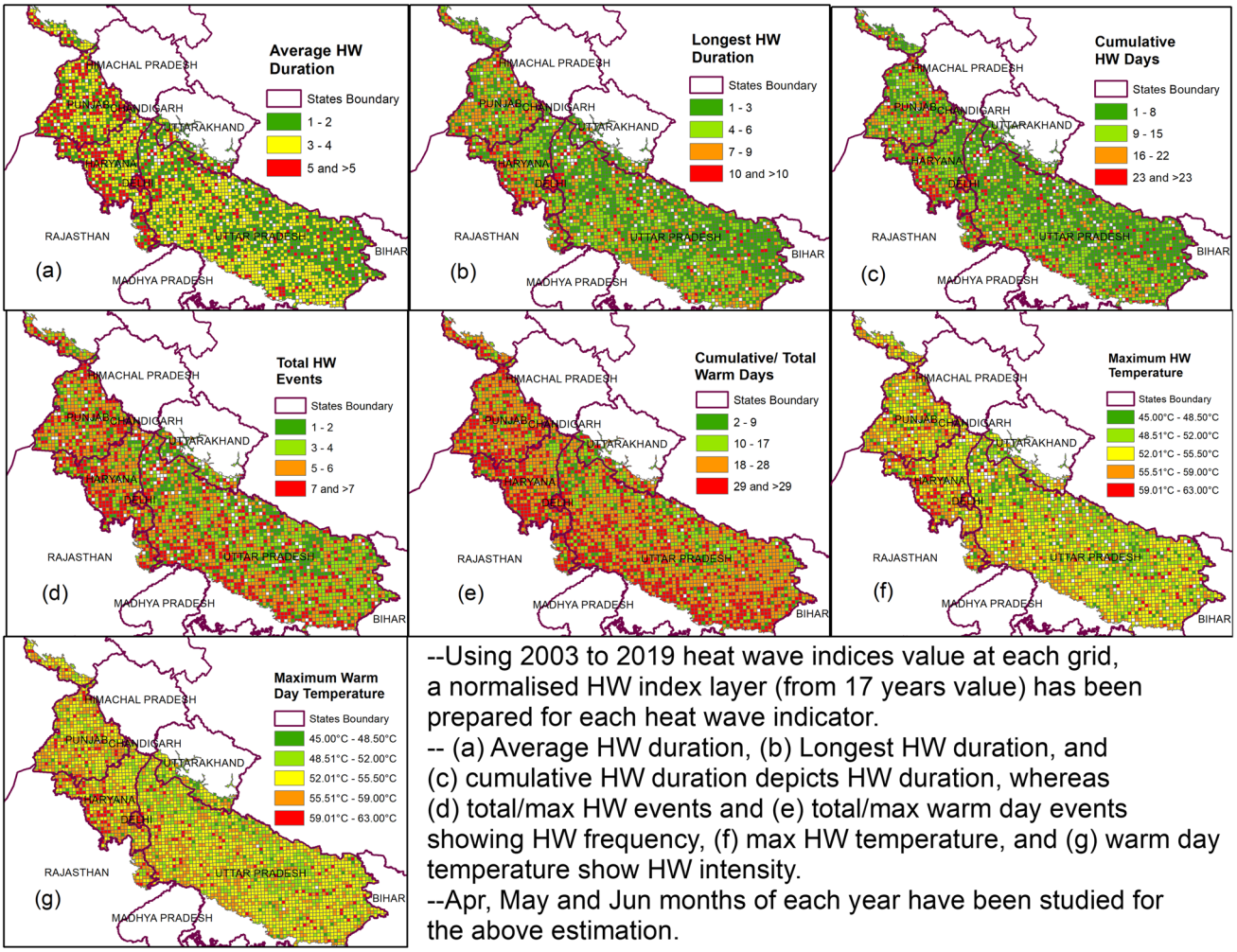

Fig. 6 Spatial distribution of each heat wave index normalised into single representative layer from 17 years of LST observation

been observed in the Uttar Pradesh and Haryana regions because of the concentrated urban centres. However, other than the NCT Delhi region, other pockets are either very small or show a scattered pattern of HW.

4.3 Change in built-up and heat wave

LULC transformation analysis of the study area revealed that built-up in 2005–2006 was 17,623.11 sq. km which increased to 20,208.30 sq. km in 2010–2011, and further to 22,406.91 sq. km in 2015–2016 (Table 4 and Fig. 11). The percentage increase of identified heat wave indicators in 2010–2011 and 2015–2016 respectively w.r.t. 2005–2006 shows a significant increase in Average HW Duration in 2015–2016 (33.33%); however, it remained nearly similar to the values in 2010–2011 as it was in 2005–2006. Similarly, Longest HW Duration increased to 25% and 125%; Cumulative HW Days increased to 12.50% and 87.50%; Total HW Events increased to 25% and 50%; increase in Total Warm Day Events recorded 10.34% and 34.48%, whereas the increase in Max HW Temperature observed is 0.24% and 3.16%, while the increase in Max Warm Day Temperature is observed as 4.92% and 8.76% in the year 2010–2011 and 2015–2016 respectively.

5 Discussion

Detailed analysis of all the identified HW indices shows that the 2010–2019 decade has been the warmer decade since each HW index displayed higher values as compared to the previous decade. However, it can also be seen (Figs. 4 and 5) that the peak of high temperature and severity of heat wave kept on fluctuating year by year as the highest range of all the indices can be visualised very clearly in some years while not so clear in others. However, the decade 2010–2019, reflects a consistent increase in the area affected by the highest and second

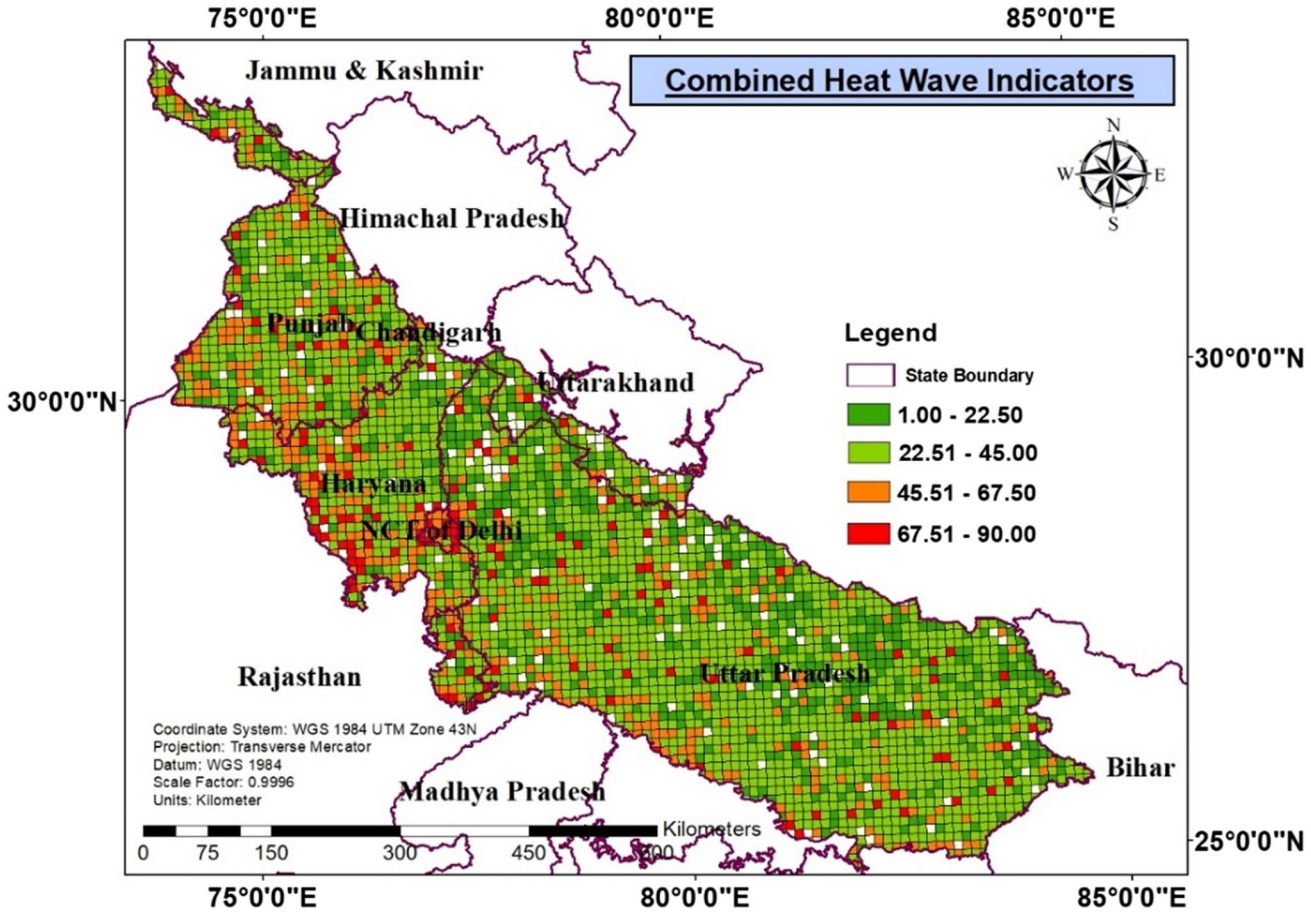

Fig. 7 Combined heat wave indicators obtained after applying AHP on seven HW indices identified for 17 years

highest range of almost all the HW indices. Change in land cover mainly from vegetation (forest, agriculture) to built-up can be considered as one of the major reasons behind this increasing phenomenon (Fig. 11). Amongst the three categories of heat wave indices, HW duration shows a significant increase from 2003 to 2019 while the HW frequency and HW intensity indices show a lesser amount of increase over the years. The increase in duration of HW is a matter of concern as consistently higher temperatures intensify the thermal discomfort and are responsible for higher mortality rates. It also points out the fact that the various climate and land use forcing are resulting in the increase in the duration of the heat wave event.

The spatial distribution of the Cumulative HW Indicator layer (Fig. 7) shows a prominent heat wave pattern in the south-western part of the study area in the state of Haryana closer to the Rajasthan border, parts of Punjab and in some scattered grids of Uttar Pradesh other than the NCT Delhi and its surrounding area. The Rajasthan region shows prominent HW due to the impact of the desert area in the western side and scarce vegetation cover and dominance of barren and fallow land (Khandelwal et al., 2018), whereas few grids in Punjab and Haryana regions show high values of Cumulative HW Indicators because of the presence of barren land and increase in built-up (Majumdar et al., 2019) which is also the case with the grids falling in the state of Uttar Pradesh in the south-western part of the study area (Singh & Verma, 2017). Lower temperature values of grids in the Uttar Pradesh region in the north-eastern side are due to the availability of extensive irrigation facilities in this area which led to the dominance of agricultural areas having high soil moisture content. Impact of built-up change is prominently seen in the grids covering Delhi (capital of India) and surrounding region as this region shows very high temperature range consistently throughout the years because of the presence of dense urban and built-up area with very little or no green space (Chakraborty et al., 2014). These observations can be also linked with the agro-climatic zones in the study area (Fig. 2), as the NCT

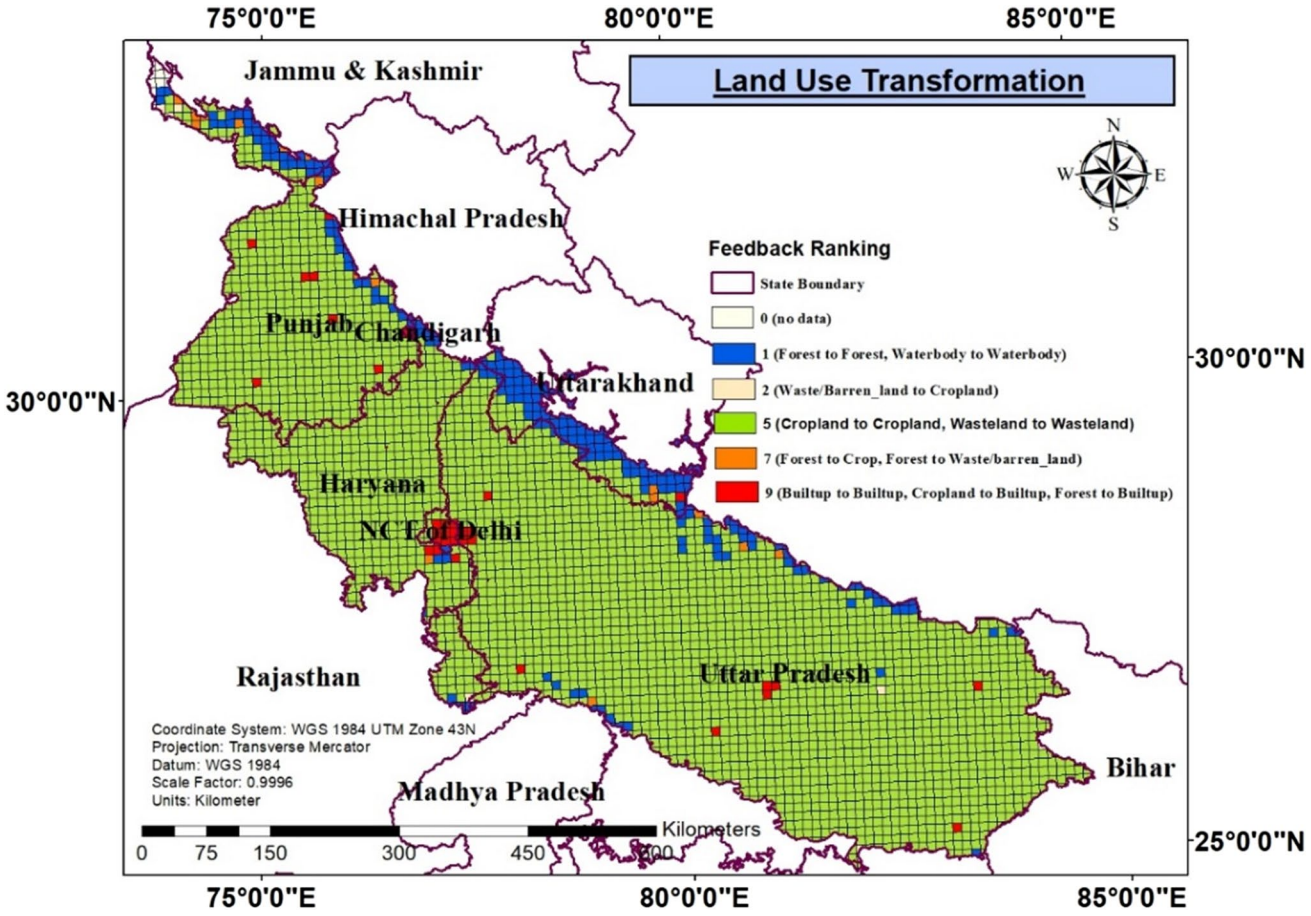

Fig. 8 Land use transformation from 2005–2006 to 2015–2016 prepared using AWiFS LULC downloaded from Bhuvan

Delhi and its surrounding witness the semi-arid type of climatic conditions with hot weather during summers. Also, the region of Uttar Pradesh contains few pockets with high HW risk and vulnerability as this region also has somewhat similar climate characteristics but because of the presence of vegetation, type of land use, and built-up and population density, the impact is somewhat less compared to the identified risk and vulnerability hotspot (NCT Delhi and its surrounding area).

It is clearly observed that land cover especially vegetation type, cropping patterns and change in built-up cover play an important role in the spatial distribution of the hotspots of HW in the Indo-Gangetic Plains. The region is dominated by the dry deciduous forest which is generally leafless during the months of April to June (Roy et al., 2012). Furthermore, the dominant land use of the region is rain-fed cropland (Kharif) which results in dominance of fallow land in this region during peak summer months (Apr–Jun). All these conditions result in a landscape devoid of green cover having very low evapotranspiration, which results in a significant high temperature regime with no mechanism to moderate the weather extreme. Furthermore, due to an increase in the built-up, there is a reduction in pervious, leading to the increased albedo. This provides a positive feedback to the temperature resulting in an increase in the heat wave conditions.

The risk and vulnerability layer after combining all HW indices, LULC transformation and population shows a maximum number of grids with highest heat wave range in and around the state of Delhi and its southern regions around the Aravalli Range. Few scattered grids of risk and vulnerability w.r.t. heat waves could be seen in other parts of the study area, but Delhi and its surrounding region spreads over a number of grids and stands out as one of the major risks and vulnerability hotspot w.r.t. heat wave. It can be majorly attributed to significant LULC changes and ongoing urbanisation, which has led to an increase in all indices in this region.

HW has become more consistent and prominent, as built-up increases in size and density turning into an

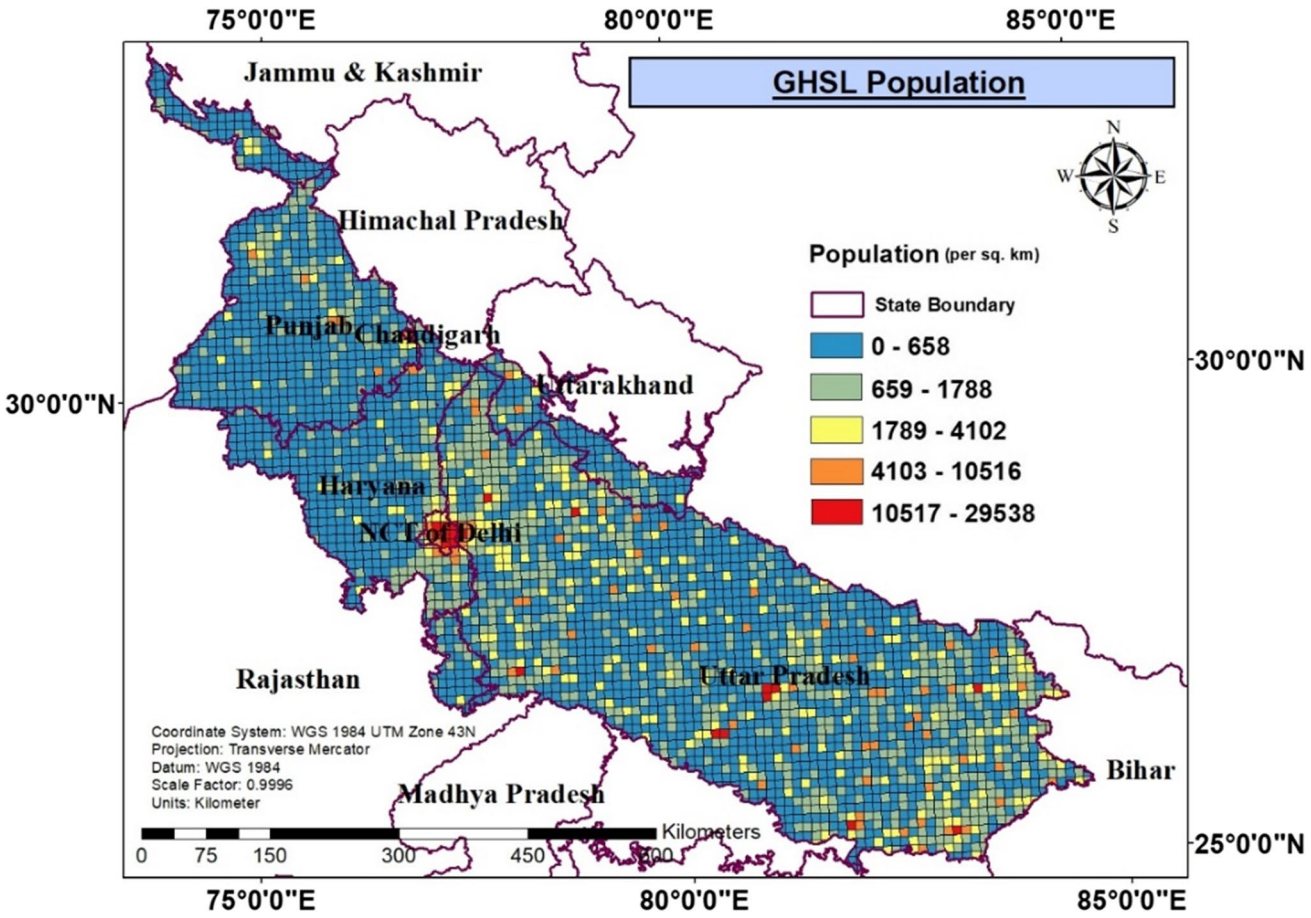

Fig. 9 Population (grid wise) derived from European Commission Global Human Settlement

urban area. Increase in dense built-up replaces natural vegetation or landscape by impervious surface in the form of buildings, roads and other structures; it leads to changes in the microclimate generally known as the UHI effect. An increase in temperature because of the local UHI phenomenon in densely built-up urban regions exaggerates the discomfort of the residents and puts them at a high level of thermal stress due to combined impact of UHI and HW (Lee et al., 2017; Steeneveld et al., 2011) which makes them more vulnerable.

GEE has served as a highly beneficial platform in this study for analysis of the large volume of earth observation (EO) LST data is used to compute HW indicators and to identify HW risk and vulnerability hotspot. Since GEE provides multiple products in analysis-ready format, it is going to revolutionise the use of EO products and has a great potential for a large number of EO applications.

6 Conclusion

This study presents an approach for spatio-temporal analysis of MODIS LST data available on GEE platform for computation and analysis of HW indicators in order to identify HW risk and vulnerability hotspot using EO data in IGPs of India. The study has dwell into understanding the spatio-temporal variability of HW in the western IGPs as well as its trend during 2003 to 2019 in a geospatial domain. The work, which is the first of its kind in the Indian landscape, uses the state-of-the-art advanced algorithms in GEE platform to analyse the long-term geo-spatial data to identify the hotspots of heat wave in the study area. The study clearly highlights areas vulnerable to heat wave incidences and how the LULC as well as the associated factors like population has resulted in the identification of heat wave hotspots. Several studies have shown that extreme heat wave events are going to increase in frequency and severity in the future; hence,

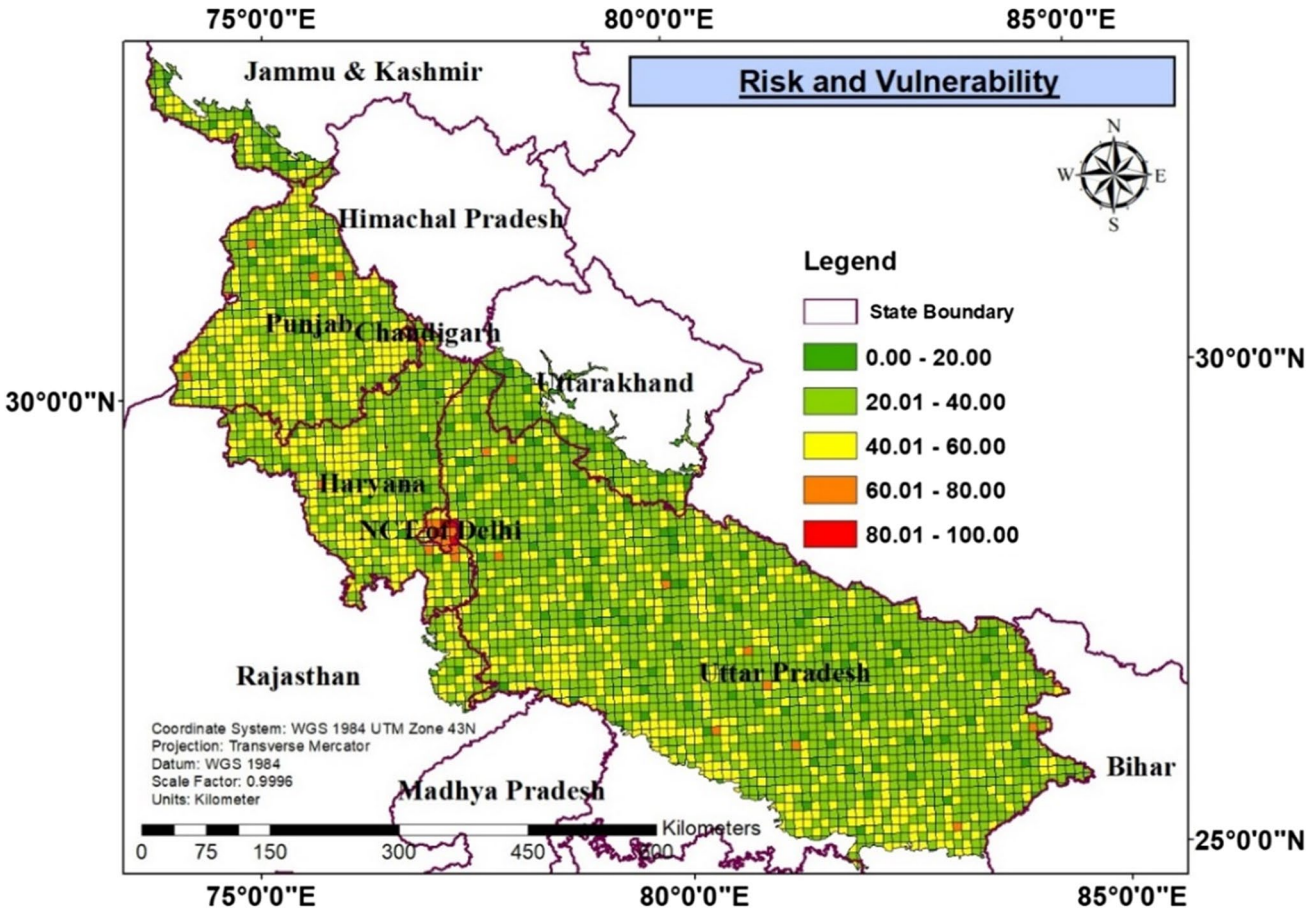

Fig. 10 Risk and vulnerability map w.r.t. heat wave and urbanisation prepared by combining all the factors with equal weightages

Table 4 Built-up area (sq. km) and heat wave indices recorded in 2005–2006, 2010–2011 and 2015–2016

Year	Area (sq. km.)	Average HW Duration	Longest HW Duration	Cumulative HW Days	Total HW Events	Total Warm Day Events	Maximum Heat Wave Temperature (°C)	Maximum Warm Day Temperature (°C)
2005–06	17,623.11	3	4	16	4	29	53.58	53.58
2010–11	20,208.30	3	5	18	5	32	53.71	56.21
2015–16	22,406.91	4	9	30	6	39	55.27	58.27

research emphasis is required on HWs and their health impacts in this less explored region. Since the population residing in IGP is significant in number (nearly 1/7th of the total population), the analysis of risk and vulnerabilities and HW trends has the potential to provide critical inputs to the stakeholders and policy-makers for framing strategies for management and mitigation of HW in the future.

In this study, MODIS LST data has been used as a proxy for ground-based measurement of ambient air temperature due to poor spatial coverage of ground data. The use of LST as a proxy may lead to some fluctuations from the actual ambient temperature as LST is usually higher than the ambient air temperature especially in non-vegetated areas, but LST can only provide spatial variation in the temperature regimes and has been used as a reliable proxy in several heat wave–related studies (Bahi et al., 2016; Good et al., 2017; Kawashima et al., 2000). However, an extensive network of ground-based observations may be able to improve the models for better projection and pattern establishment. The work can be taken further by incorporating data on relative

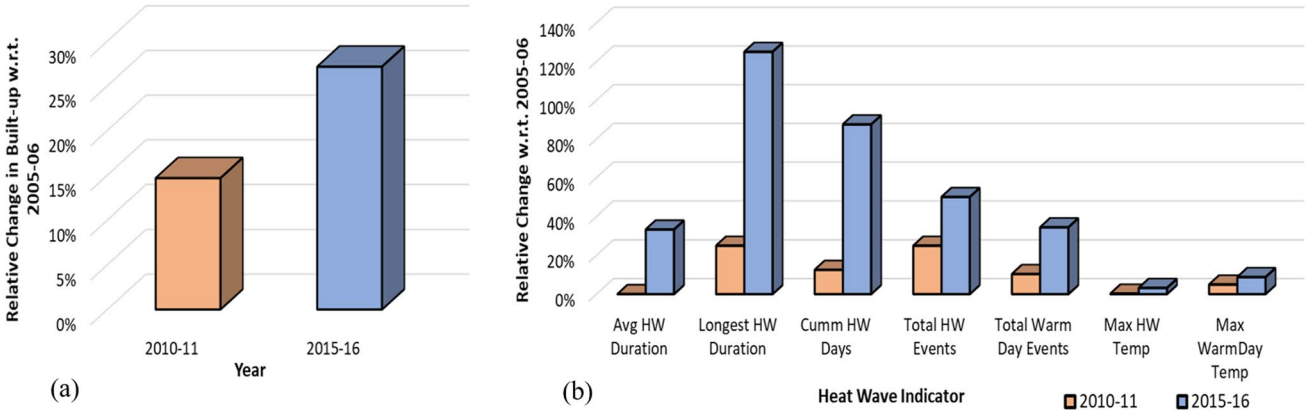

Fig. 11 Relative percentage increase of (**a**) built-up area, and (**b**) heat wave indices, in the year 2010–2011 and 2015–2016 w.r.t. the year 2005–2006

humidity (RH) in the analysis as RH plays a major role in the heat wave exposure and thermal comfort level for humans (Pal & Eltahir, 2016).

The work reported is original and has not been published elsewhere, nor is it currently under consideration for publication elsewhere.

Acknowledgements The authors are thankful to Director IIRS and Chairman ISRO for the encouragement and facilitating the work. The work has been carried out as part of the M. Tech. Dissertation work. The EO data from USGS, GHSL, Bhuvan and Google Earth Engine is acknowledged.

Author contribution All authors whose names appear on the submission have made substantial contributions to the conception or design of the work; the acquisition, analysis, or interpretation of data; or the creation of code used in the work. All authors agree to be accountable for all aspects of the work in ensuring that questions related to the accuracy or integrity of any part of the work are appropriately investigated and resolved.

Data availability The findings of the study were derived from the openly available dataset from following resources available in the public domain: [Aqua MODIS daily LST (https://earthengine.google.com/platform/), temporal LULC map (https://bhuvan-app1.nrsc.gov.in/thematic/thematic/index.php#), and population data from Global Human Settlement Layer (GHSL) (https://ghsl.jrc.ec.europa.eu/download.php?ds=pop)]. Derived data that support the findings of this study are available on request from the corresponding author (Gupta K.)

Code availability Code developed as part of this study is a copyright material of the Indian Institute of Remote Sensing, ISRO, India. It can be shared to interested researchers on request by the corresponding author (Gupta K.).

Declarations

Ethics approval The work is carried out at the Indian Institute of Remote Sensing/ISRO, Dehradun, as part of ongoing research. All datasets used in this study area available in public domain from the following resources: Aqua MODIS daily LST (https://earthengine.google.com/platform/), temporal LULC map (https://bhuvan-app1.nrsc.gov.in/thematic/thematic/index.php#) and population data from Global Human Settlement Layer (GHSL) (https://ghsl.jrc.ec.europa.eu/download.php?ds=pop). All the research articles has been cited appropriately in the manuscript as per the defined style and format.

Consent to participate Consent to participate is not applicable for this study and it is entirely based on analysis of spatial data and does not include any human or live participants.

Consent for publication Consent for publication is not applicable as no human or live participant has been utilised to carry out this study.

Conflict of interest The authors declare no competing interests.

References

Alexander LV, Zhang X, Peterson TC, Caesar J, Gleason B, Klein Tank AMG, Haylock M, Collins D, Trewin B, Rahimzadeh F, Tagipour A, Rupa Kumar K, Revadekar J, Griffiths G, Vincent L, Stephenson DB, Burn J, Aguilar E, Brunet M, Taylor M, New M, Zhai P, Rusticucci M, Vazquez-Aguirre JL (2006) Global observed changes in daily climate extremes of temperature and precipitation. J Geophys Res Atmos 111(5):1–22. https://doi.org/10.1029/2005JD006290

Bahi H, Rhinane H, Bensalmia A (2016) Contribution of MODIS satellite image to estimate the daily air temperature in the Casablanca City, Morocco. Int Arch Photogramm Remote Sens Spat Inf Sci - ISPRS Arch 42(2W1):3–11. https://doi.org/10.5194/isprs-archives-XLII-2-W1-3-2016

Balan R, Rao P, Gupta K, Roy A. (2020) Open source Google Earth Platform for computation of heat wave indicators, FOSS4G Korea 2020, 12–13 November, 2020, Seoul, Korea, Retrieved from https://foss4g.osgeo.kr/slides/english01/PriyankaRao_FOSS4G_Korea_2020.pdf. Accessed 21 Jun 2021

Barriopedro D, Fischer EM, Luterbacher J, Trigo RM, García-Herrera R (2011) The hot summer of 2010: redrawing the temperature record map of Europe. Science 332(6026):220–224. https://doi.org/10.1126/science.1201224

Chakraborty S, Kant Y, Bharath B. (2014) Study of land surface temperature in Delhi City to manage the thermal effect on urban

developments. International Journal of Advanced Scientific and Technical Research, 1(4), 439–450. Retrieved from http://www.rspublication.com/ijst/index.html%0AIssue. Accessed 14 May 2021

Christidis N, Stott PA, Brown SJ (2011) The role of human activity in the recent warming of extremely warm daytime temperatures. J Clim 24(7):1922–1930. https://doi.org/10.1175/2011JCLI4150.1

Conti S, Meli P, Minelli G, Solimini R, Toccaceli V, Vichi M, Beltrano MC, Perini L (2005) Epidemiologic study of mortality during summer 2003 in Italian regional capitals: Results of a rapid survey. Extreme Weather Events and Public Health Responses 109–120. https://doi.org/10.1007/3-540-28862-7_11

Darryn M, Iftekhar A, Jane M (2012) The impact of the 2009 heat wave on Melbourne's critical infrastructure. Local Environ 17(8):783–796. https://doi.org/10.1080/13549839.2012.678320

Eckstein D, Kunzel V, Schafer L, Winges M. (2019) Global climate risk index 2020. In J. Chapman-Rose & J. Longwitz (Eds.), *Berlin: Germanwatch*. Retrieved from www.germanwatch.org/en/cri. Accessed 20 Jul 2020

Frich P, Alexander LV, Della-Marta P, Gleason B, Haylock M, Tank Klein AMG, Peterson T (2002) Observed coherent changes in climatic extremes during the second half of the twentieth century. Clim Res 19(3):193–212. https://doi.org/10.3354/cr019193

Ghosh S (2020) India's hot climate got hotter in the past decade. Retrieved from https://qz.com/india/1819028/indias-hot-climate-got-hotter-in-the-past-decade/. Accessed 10 Oct 2020

Good EJ, Ghent DJ, Bulgin CE, Remedios JJ (2017) A spatiotemporal analysis of the relationship between near-surface air temperature and satellite land surface temperatures using 17 years of data from the ATSR series. Journal of Geophysical Research: Atmospheres 122(17):9185–9210. https://doi.org/10.1002/2017JD026880

IMD (2019) Statement on climate of India during 2019: temperatures. In *Ministry of Earth Sciences*. Retrieved from https://public.wmo.int/en/resources/library/wmo-provisional-statement-state-of-global-climate-2019. Accessed 10 Oct 2020

Intergovernmental Panel on Climate Change. (2007). Climate change 2007 impacts, adaptation and vulnerability. In (Cambridge University Press Ed.). UK. https://doi.org/10.1029/93JC02439

Kawashima S, Ishida T, Minomura M, Miwa T (2000) Relations between surface temperature and air temperature on a local scale during winter nights. J Appl Meteorol 39(9):1570–1579. https://doi.org/10.1175/1520-0450(2000)039%3c1570:RBSTAA%3e2.0.CO;2

Khandelwal S, Goyal R, Kaul N, Mathew A (2018) Assessment of land surface temperature variation due to change in elevation of area surrounding Jaipur, India. Egypt J Remote Sens Space Sci 21(1):87–94. https://doi.org/10.1016/j.ejrs.2017.01.005

Khan N, Shahid S, Ismail T, Ahmed K, Nawaz N (2019) Trends in heat wave related indices in Pakistan. Stoch Environ Res Risk Assess 33(1):287–302. https://doi.org/10.1007/s00477-018-1605-2

Lee, Y. Y., Md Din, M. F., Ponraj, M., Noor, Z. Z., Iwao, K., & Chelliapan, S. (2017). Overview of urban heat island (UHI) phenomenon towards human thermal comfort. Environ Eng Manag J 16(9):2097–2112. https://doi.org/10.30638/eemj.2017.217

Luo L, Zhang Y (2012) Did we see the 2011 summer heat wave coming? Geophys Res Lett 39(9):1–5. https://doi.org/10.1029/2012GL05138

Majumdar A, Kingra PK, Setia R, Singh SP, Pateriya B (2019) Influence of land use/land cover changes on surface temperature and its effect on crop yield in different agro-climatic regions of Indian Punjab. Geocarto Int. https://doi.org/10.1080/10106049.2018.1520927

Mandal DK, Mandal C, Singh SK (2016) Delineating agro-ecological regions. National Bureau of Soil Survey and Land Use Planning, 1–8. https://www.nbsslup.in/assets/uploads/clinks/DelineatingAgro-EcologicalRegions.pdf. Accessed 10 Jun 2021

Mazdiyasni O, Sadegh M, Chiang F, AghaKouchak A (2019) Heat wave Intensity Duration Frequency Curve: A multivariate approach for hazard and attribution analysis. In Scientific Reports (Vol. 9). https://doi.org/10.1038/s41598-019-50643-w

Meehl GA, Tebaldi C (2004) More intense, more frequent, and longer lasting heat waves in the 21st century. Science 305(5686):994–997. https://doi.org/10.1126/science.1098704

Miralles DG, Gentine P, Seneviratne SI, Teuling AJ (2019) Land–atmospheric feedbacks during droughts and heatwaves: state of the science and current challenges. Ann N Y Acad Sci 1436(1):19–35. https://doi.org/10.1111/nyas.13912

Mishra V, Mukherjee S, Kumar R, Stone DA (2017) Heat wave exposure in India in current, 1.5 °c, and 2.0 °c worlds. Environ Res Lett 12(12). https://doi.org/10.1088/1748-9326/aa9388

National Remote Sensing Agency, H. (2007) National land use and land cover mapping using multi-temporal AWiFS data (Issue June). Accessed on June 14, 2021 from https://bhuvan-app1.nrsc.gov.in/2dresources/thematic/LULC250/0506.pdf

National Remote Sensing Centre, H. (2010). National land use and land cover mapping using multi-temporal AWiFS data. Accessed on June 14, 2021 from https://bhuvan-app1.nrsc.gov.in/2dresources/thematic/LULC250/0809.pdf

Pai DS, Nair SA, Ramanathan AN (2013) Long term climatology and trends of heat waves over India during the recent 50 years (1961–2010). *Mausam*, *64*(4), 585–604. Retrieved from http://metnet.imd.gov.in/mausamdocs/16441_F.pdf. Accessed 20 Jul 2020

Pal JS, Eltahir EAB (2016) Future temperature in southwest Asia projected to exceed a threshold for human adaptability. Nat Clim Chang 6(2):197–200. https://doi.org/10.1038/nclimate2833

Panda DK, AghaKouchak A, Ambast SK (2017) Increasing heat waves and warm spells in India, observed from a multiaspect framework. J Geophys Res 122(7):3837–3858. https://doi.org/10.1002/2016JD026292

Papanastasiou DK, Melas D, Kambezidis HD (2014) Heat waves characteristics and their relation to air quality in Athens. Glob. Nest J 16(5):919–928. https://doi.org/10.30955/gnj.001530

Perkins SE (2011) Biases and model agreement in projections of climate extremes over the tropical Pacific. Earth Interact 15(24):1–36. https://doi.org/10.1175/2011EI395.1

Rathee G (2014) Trends of land-use change in India. In Urbanization in Asia: Governance, Infrastructure and The Environment (pp. 215–238). https://doi.org/10.1007/978-81-322-1638-4_13

Rodgers WA, Panwar SH (1988) Planning a wildlife protected area network in India. FAO Accession No: XF9093847, FAO/Wildlife Institute of India, Dehradun India

Rohini P, Rajeevan M, Srivastava AK (2016) On the Variability and Increasing Trends of Heat Waves over India. Scientific Reports, 6(June). https://doi.org/10.1038/srep26153

Roy S, Byrne J, Pickering C (2012) A systematic quantitative review of urban tree benefits, costs, and assessment methods across cities in different climatic zones. Urban For Urban Green 11(4):351–363. https://doi.org/10.1016/j.ufug.2012.06.006

Seneviratne SI, Nicholls N, Easterling D, Goodess CM, Kanae S, Kossin J, Luo Y, Marengo J, Mclnnes K, Rahimi M, Rahimi M, Reichstein M, Sorteberg A, Vera C, Zhang X (2012) Changes in climate extremes and their impacts on the natural physical environment. In Managing the Risks of Extreme Events and Disasters to Advance Climate Change Adaptation (pp. 109–230).

Shafiei Shiva J, Chandler DG, Kunkel KE (2019) Localized Changes in Heat Wave Properties Across the United States. Earth's Future 7(3):300–319. https://doi.org/10.1029/2018EF001085

Shelestov A, Lavreniuk M, Kussul N, Novikov A, Skakun S (2017) Exploring Google Earth Engine platform for big data processing: classification of multi-temporal satellite imagery for crop

mapping. Front Earth Sci 5(February):1–10. https://doi.org/10.3389/feart.2017.00017

Singh P, Verma P (2017) Impact of land use change and urbanization on urban heat island in Lucknow City, Central India. A remote sensing based estimate. Sustainable Cities and Society. https://doi.org/10.1016/j.scs.2017.02.018

Steeneveld GJ, Koopmans S, Heusinkveld BG, Van Hove LWA, Holtslag AAM (2011) Quantifying urban heat island effects and human comfort for cities of variable size and urban morphology in the Netherlands. J Geophys Res Atmos 116(20):1–14. https://doi.org/10.1029/2011JD015988

WMO (2011) Provisional statement on the status of the global climate. Retrieved from http://www.wmo.int/pages/mediacentre/press_releases/gcs_2011_en.html. Accessed 20 Jul 2020

WMO (2018) Guidelines on the defintion and monitoring of extreme weather and climate events. Retrieved from http://www.wmo.int/pages/prog/wcp/ccl/documents/GUIDELINESONTHEDEFINTIONANDMONITORINGOFEXTREMEWEATHERANDCLIMATEEVENTS_09032018.pdf. Accessed 20 Jul 2020